

Incident energy dependence of p_t correlations at relativistic energies

J. Adams,³ M. M. Aggarwal,²⁹ Z. Ahammed,⁴³ J. Amonett,²⁰ B. D. Anderson,²⁰ D. Arkhipkin,¹³ G. S. Averichev,¹² S. K. Badyal,¹⁹ Y. Bai,²⁷ J. Balewski,¹⁷ O. Barannikova,³² L. S. Barnby,³ J. Baudot,¹⁸ S. Bekele,²⁸ V. V. Belaga,¹² A. Bellingeri-Laurikainen,³⁸ R. Bellwied,⁴⁶ J. Berger,¹⁴ B. I. Bezverkhny,⁴⁸ S. Bharadwaj,³³ A. Bhasin,¹⁹ A. K. Bhati,²⁹ V. S. Bhatia,²⁹ H. Bichsel,⁴⁵ J. Bielcik,⁴⁸ J. Bielcikova,⁴⁸ A. Billmeier,⁴⁶ L. C. Bland,⁴ C. O. Blyth,³ B. E. Bonner,³⁴ M. Botje,²⁷ A. Boucham,³⁸ J. Bouchet,³⁸ A. V. Brandin,²⁵ A. Bravar,⁴ M. Bystersky,¹¹ R. V. Cadman,¹ X. Z. Cai,³⁷ H. Caines,⁴⁸ M. Calderón de la Barca Sánchez,¹⁷ J. Castillo,²¹ O. Catu,⁴⁸ D. Cebra,⁷ Z. Chajecski,²⁸ P. Chaloupka,¹¹ S. Chattopadhyay,⁴³ H. F. Chen,³⁶ Y. Chen,⁸ J. Cheng,⁴¹ M. Cherney,¹⁰ A. Chikanian,⁴⁸ W. Christie,⁴ J. P. Coffin,¹⁸ T. M. Cormier,⁴⁶ J. G. Cramer,⁴⁵ H. J. Crawford,⁶ D. Das,⁴³ S. Das,⁴³ M. Daugherty,⁴⁰ M. M. de Moura,³⁵ T. G. Dedovich,¹² A. A. Derevschikov,³¹ L. Didenko,⁴ T. Dietel,¹⁴ S. M. Dogra,¹⁹ W. J. Dong,⁸ X. Dong,³⁶ J. E. Draper,⁷ F. Du,⁴⁸ A. K. Dubey,¹⁵ V. B. Dunin,¹² J. C. Dunlop,⁴ M. R. Dutta Mazumdar,⁴³ V. Eckardt,²³ W. R. Edwards,²¹ L. G. Efimov,¹² V. Emelianov,²⁵ J. Engelage,⁶ G. Eppley,³⁴ B. Erasmus,³⁸ M. Estienne,³⁸ P. Fachini,⁴ J. Faivre,¹⁸ R. Fatemi,¹⁷ J. Fedorisin,¹² K. Filimonov,²¹ P. Filip,¹¹ E. Finch,⁴⁸ V. Fine,⁴ Y. Fisyak,⁴ J. Fu,⁴¹ C. A. Gagliardi,³⁹ L. Gaillard,³ J. Gans,⁴⁸ M. S. Ganti,⁴³ F. Geurts,³⁴ V. Ghazikhanian,⁸ P. Ghosh,⁴³ J. E. Gonzalez,⁸ H. Gos,⁴⁴ O. Grachov,⁴⁶ O. Grebenyuk,²⁷ D. Grosnick,⁴² S. M. Guertin,⁸ Y. Guo,⁴⁶ A. Gupta,¹⁹ T. D. Gutierrez,⁷ T. J. Hallman,⁴ A. Hamed,⁴⁶ D. Hardtke,²¹ J. W. Harris,⁴⁸ M. Heinz,² T. W. Henry,³⁹ S. Hepplemann,³⁰ B. Hippolyte,¹⁸ A. Hirsch,³² E. Hjort,²¹ G. W. Hoffmann,⁴⁰ H. Z. Huang,⁸ S. L. Huang,³⁶ E. W. Hughes,⁵ T. J. Humanic,²⁸ G. Igo,⁸ A. Ishihara,⁴⁰ P. Jacobs,²¹ W. W. Jacobs,¹⁷ M. Jedynek,⁴⁴ H. Jiang,⁸ P. G. Jones,³ E. G. Judd,⁶ S. Kabana,² K. Kang,⁴¹ M. Kaplan,⁹ D. Keane,²⁰ A. Kechechyan,¹² V. Yu. Khodyrev,³¹ J. Kiryluk,²² A. Kisiel,⁴⁴ E. M. Kislov,¹² J. Klay,²¹ S. R. Klein,²¹ D. D. Koetke,⁴² T. Kollegger,¹⁴ M. Kopytine,²⁰ L. Kotchenda,²⁵ K. L. Kowalik,²¹ M. Kramer,²⁶ P. Kravtsov,²⁵ V. I. Kravtsov,³¹ K. Krueger,¹ C. Kuhn,¹⁸ A. I. Kulikov,¹² A. Kumar,²⁹ R. Kh. Kutuev,¹³ A. A. Kuznetsov,¹² M. A. C. Lamont,⁴⁸ J. M. Landgraf,⁴ S. Lange,¹⁴ F. Laue,⁴ J. Lauret,⁴ A. Lebedev,⁴ R. Lednicky,¹² S. Lehocka,¹² M. J. LeVine,⁴ C. Li,³⁶ Q. Li,⁴⁶ Y. Li,⁴¹ G. Lin,⁴⁸ S. J. Lindenbaum,²⁶ M. A. Lisa,²⁸ F. Liu,⁴⁷ H. Liu,³⁶ L. Liu,⁴⁷ Q. J. Liu,⁴⁵ Z. Liu,⁴⁷ T. Ljubicic,⁴ W. J. Llope,³⁴ H. Long,⁸ R. S. Longacre,⁴ M. Lopez-Noriega,²⁸ W. A. Love,⁴ Y. Lu,⁴⁷ T. Ludlam,⁴ D. Lynn,⁴ G. L. Ma,³⁷ J. G. Ma,⁸ Y. G. Ma,³⁷ D. Magestro,²⁸ S. Mahajan,¹⁹ D. P. Mahapatra,¹⁵ R. Majka,⁴⁸ L. K. Mangotra,¹⁹ R. Manweiler,⁴² S. Margetis,²⁰ C. Markert,²⁰ L. Martin,³⁸ J. N. Marx,²¹ H. S. Matis,²¹ Yu. A. Matulenko,³¹ C. J. McClain,¹ T. S. McShane,¹⁰ F. Meissner,²¹ Yu. Melnick,³¹ A. Meschanin,³¹ M. L. Miller,²² N. G. Minaev,³¹ C. Mironov,²⁰ A. Mischke,²⁷ D. K. Mishra,¹⁵ J. Mitchell,³⁴ B. Mohanty,⁴³ L. Molnar,³² C. F. Moore,⁴⁰ D. A. Morozov,³¹ M. G. Munhoz,³⁵ B. K. Nandi,⁴³ S. K. Nayak,¹⁹ T. K. Nayak,⁴³ J. M. Nelson,³ P. K. Netrakanti,⁴³ V. A. Nikitin,¹³ L. V. Nogach,³¹ S. B. Nurushev,³¹ G. Odyniec,²¹ A. Ogawa,⁴ V. Okorokov,²⁵ M. Oldenburg,²¹ D. Olson,²¹ S. K. Pal,⁴³ Y. Panebratsev,¹² S. Y. Panitkin,⁴ A. I. Pavlinov,⁴⁶ T. Pawlak,⁴⁴ T. Peitzmann,²⁷ V. Perevoztchikov,⁴ C. Perkins,⁶ W. Peryt,⁴⁴ V. A. Petrov,⁴⁶ S. C. Phatak,¹⁵ R. Picha,⁷ M. Planinic,⁴⁹ J. Pluta,⁴⁴ N. Porile,³² J. Porter,⁴⁵ A. M. Poskanzer,²¹ M. Potekhin,⁴ E. Potrebenikova,¹² B. V. K. S. Potukuchi,¹⁹ D. Prindle,⁴⁵ C. Pruneau,⁴⁶ J. Putschke,²¹ G. Rakness,³⁰ R. Raniwala,³³ S. Raniwala,³³ O. Ravel,³⁸ R. L. Ray,⁴⁰ S. V. Razin,¹² D. Reichhold,³² J. G. Reid,⁴⁵ J. Reinharth,³⁸ G. Renault,³⁸ F. Retiere,²¹ A. Ridiger,²⁵ H. G. Ritter,²¹ J. B. Roberts,³⁴ O. V. Rogachevskiy,¹² J. L. Romero,⁷ A. Rose,²¹ C. Roy,³⁸ L. Ruan,³⁶ M. Russcher,²⁷ R. Sahoo,¹⁵ I. Sakrejda,²¹ S. Salur,⁴⁸ J. Sandweiss,⁴⁸ M. Sarsour,¹⁷ I. Savin,¹³ P. S. Sazhin,¹² J. Schambach,⁴⁰ R. P. Scharenberg,³² N. Schmitz,²³ K. Schweda,²¹ J. Seger,¹⁰ P. Seyboth,²³ E. Shahaliev,¹² M. Shao,³⁶ W. Shao,⁵ M. Sharma,²⁹ W. Q. Shen,³⁷ K. E. Shestermanov,³¹ S. S. Shimanskiy,¹² E. Sichtermann,²¹ F. Simon,²³ R. N. Singaraju,⁴³ N. Smirnov,⁴⁸ R. Snellings,²⁷ G. Sood,⁴² P. Sorensen,²¹ J. Sowinski,¹⁷ J. Speltz,¹⁸ H. M. Spinka,¹ B. Srivastava,³² A. Stadnik,¹² T. D. S. Stanislaus,⁴² R. Stock,¹⁴ A. Stolpovsky,⁴⁶ M. Strikhanov,²⁵ B. Stringfellow,³² A. A. P. Suaide,³⁵ E. Sugarbaker,²⁸ C. Suire,⁴ M. Sumera,¹¹ B. Surrow,²² M. Swanger,¹⁰ T. J. M. Symons,²¹ A. Szanto de Toledo,³⁵ A. Tai,⁸ J. Takahashi,³⁵ A. H. Tang,²⁷ T. Tarnowsky,³² D. Thein,⁸ J. H. Thomas,²¹ S. Timoshenko,²⁵ M. Tokarev,¹² S. Trentalange,⁸ R. E. Tribble,³⁹ O. D. Tsai,⁸ J. Ulery,³² T. Ullrich,⁴ D. G. Underwood,¹ G. Van Buren,⁴ M. van Leeuwen,²¹ A. M. Vander Molen,²⁴ R. Varma,¹⁶ I. M. Vasilevski,¹³ A. N. Vasiliev,³¹ R. Vernet,¹⁸ S. E. Vigdor,¹⁷ Y. P. Viyogi,⁴³ S. Vokal,¹² S. A. Voloshin,⁴⁶ W. T. Waggoner,¹⁰ F. Wang,³² G. Wang,²⁰ G. Wang,⁵ X. L. Wang,³⁶ Y. Wang,⁴⁰ Y. Wang,⁴¹ Z. M. Wang,³⁶ H. Ward,⁴⁰ J. W. Watson,²⁰ J. C. Webb,¹⁷ G. D. Westfall,²⁴ A. Wetzler,²¹ C. Whitten Jr.,⁸ H. Wieman,²¹ S. W. Wissink,¹⁷ R. Witt,² J. Wood,⁸ J. Wu,³⁶ N. Xu,²¹ Z. Xu,⁴ Z. Z. Xu,³⁶ E. Yamamoto,²¹ P. Yepes,³⁴ V. I. Yurevich,¹² I. Zborovsky,¹¹ H. Zhang,⁴ W. M. Zhang,²⁰ Y. Zhang,³⁶ Z. P. Zhang,³⁶ R. Zoukarneev,¹³ Y. Zoukarneeva,¹³ and A. N. Zubarev¹²

(STAR Collaboration)

¹Argonne National Laboratory, Argonne, Illinois 60439, USA²University of Bern, CH-3012 Bern, Switzerland³University of Birmingham, Birmingham, United Kingdom⁴Brookhaven National Laboratory, Upton, New York 11973, USA⁵California Institute of Technology, Pasadena, California 91125, USA⁶University of California, Berkeley, California 94720, USA⁷University of California, Davis, California 95616, USA⁸University of California, Los Angeles, California 90095, USA⁹Carnegie Mellon University, Pittsburgh, Pennsylvania 15213, USA

- ¹⁰Creighton University, Omaha, Nebraska 68178, USA
¹¹Nuclear Physics Institute AS CR, 250 68 Řež/Prague, Czech Republic
¹²Laboratory for High Energy, Dubna, Russia
¹³Particle Physics Laboratory, Dubna, Russia
¹⁴University of Frankfurt, Frankfurt, Germany
¹⁵Institute of Physics, Bhubaneswar 751005, India
¹⁶Indian Institute of Technology, Mumbai, India
¹⁷Indiana University, Bloomington, Indiana 47408, USA
¹⁸Institut de Recherches Subatomiques, Strasbourg, France
¹⁹University of Jammu, Jammu 180001, India
²⁰Kent State University, Kent, Ohio 44242, USA
²¹Lawrence Berkeley National Laboratory, Berkeley, California 94720, USA
²²Massachusetts Institute of Technology, Cambridge, Massachusetts 02139-4307, USA
²³Max-Planck-Institut für Physik, Munich, Germany
²⁴Michigan State University, East Lansing, Michigan 48824, USA
²⁵Moscow Engineering Physics Institute, Moscow, Russia
²⁶City College of New York, New York City, New York 10031, USA
²⁷NIKHEF and Utrecht University, Amsterdam, The Netherlands
²⁸Ohio State University, Columbus, Ohio 43210, USA
²⁹Panjab University, Chandigarh 160014, India
³⁰Pennsylvania State University, University Park, Pennsylvania 16802, USA
³¹Institute of High Energy Physics, Protvino, Russia
³²Purdue University, West Lafayette, Indiana 47907, USA
³³University of Rajasthan, Jaipur 302004, India
³⁴Rice University, Houston, Texas 77251, USA
³⁵Universidade de São Paulo, São Paulo, Brazil
³⁶University of Science & Technology of China, Anhui 230027, China
³⁷Shanghai Institute of Applied Physics, Shanghai 201800, China
³⁸SUBATECH, Nantes, France
³⁹Texas A&M University, College Station, Texas 77843, USA
⁴⁰University of Texas, Austin, Texas 78712, USA
⁴¹Tsinghua University, Beijing 100084, China
⁴²Valparaiso University, Valparaiso, Indiana 46383, USA
⁴³Variable Energy Cyclotron Centre, Kolkata 700064, India
⁴⁴Warsaw University of Technology, Warsaw, Poland
⁴⁵University of Washington, Seattle, Washington 98195, USA
⁴⁶Wayne State University, Detroit, Michigan 48201, USA
⁴⁷Institute of Particle Physics, CCNU (HZNU), Wuhan 430079, China
⁴⁸Yale University, New Haven, Connecticut 06520, USA
⁴⁹University of Zagreb, Zagreb, HR-10002, Croatia
- (Received 25 April 2005; published 19 October 2005)

We present results for two-particle transverse momentum correlations, $\langle \Delta p_{t,i} \Delta p_{t,j} \rangle$, as a function of event centrality for Au+Au collisions at $\sqrt{s_{NN}} = 20, 62, 130,$ and 200 GeV at the BNL Relativistic Heavy Ion Collider. We observe correlations decreasing with centrality that are similar at all four incident energies. The correlations multiplied by the multiplicity density increase with incident energy, and the centrality dependence may show evidence of processes such as thermalization, jet production, or the saturation of transverse flow. The square root of the correlations divided by the event-wise average transverse momentum per event shows little or no beam energy dependence and generally agrees with previous measurements made at the CERN Super Proton Synchrotron.

DOI: [10.1103/PhysRevC.72.044902](https://doi.org/10.1103/PhysRevC.72.044902)

PACS number(s): 25.75.Gz

The study of event-by-event fluctuations in global quantities, which are intimately related to correlations in particle production, may provide evidence for the production of quark-gluon plasma (QGP) in relativistic heavy-ion collisions [1–15]. Various theoretical works predict that the production of a

QGP phase in relativistic heavy-ion collisions could produce significant dynamic event-by-event fluctuations in apparent temperature, mean transverse momentum, multiplicity, and conserved quantities such as net charge. Several recent experimental studies at the CERN Super Proton Synchrotron (SPS)

[16–18] and at the BNL Relativistic Heavy Ion Collider (RHIC) [19–24] have focused on the study of fluctuations and correlations in relativistic heavy-ion collisions. One possible signal of the QGP would be a nonmonotonic change in p_t correlations as a function of centrality and/or as the incident energy is raised [8].

Here we report an experimental study of the incident energy dependence of p_t correlations we obtained by using Au+Au collisions ranging in center-of-mass energy from the highest SPS energy to the highest RHIC energy, which we measured by using the solenoidal tracker at RHIC (STAR) detector.

Fluctuations involve a purely statistical component arising from the stochastic nature of particle production and detection processes, as well as a dynamic component determined by correlations arising in various particle production processes. In this paper we first unambiguously demonstrate the existence of a finite dynamical component at all four incident energies by comparing the distribution of measured event-wise average transverse momentum per event, $\langle p_t \rangle$, with the same quantity from mixed events. We then analyze these dynamical fluctuations by using the two-particle transverse momentum correlations defined as covariance,

$$\langle \Delta p_{t,i} \Delta p_{t,j} \rangle = \frac{1}{N_{\text{event}}} \sum_{k=1}^{N_{\text{event}}} \frac{C_k}{N_k(N_k - 1)}, \quad (1)$$

where

$$C_k = \sum_{i=1}^{N_k} \sum_{j=1, i \neq j}^{N_k} (p_{t,i} - \langle p_t \rangle)(p_{t,j} - \langle p_t \rangle), \quad (2)$$

N_{event} is the number of events, $p_{t,i}$ is the transverse momentum of the i th track in each event, and N_k is the number of tracks in the k th event. The overall event average transverse momentum $\langle \langle p_t \rangle \rangle$ is given by

$$\langle \langle p_t \rangle \rangle = \left(\sum_{k=1}^{N_{\text{event}}} \langle p_t \rangle_k \right) / N_{\text{event}}, \quad (3)$$

where $\langle p_t \rangle_k$ is the average transverse momentum per event given by

$$\langle p_t \rangle_k = \left(\sum_{i=1}^{N_k} p_{t,i} \right) / N_k. \quad (4)$$

$\langle \Delta p_{t,i} \Delta p_{t,j} \rangle$ is independent, to first order, of detection efficiencies because both the numerator C_k and the denominator $N_k(N_k - 1)$ are proportional to the square of the particle detection efficiency. Therefore the efficiency cancels. By construction, $\langle \Delta p_{t,i} \Delta p_{t,j} \rangle$ is zero within statistics for properly mixed events because all correlations are removed. Note that we use mixed events only in Fig. 1.

We measured the data used in this analysis by using the solenoidal tracker at RHIC (STAR) detector to study Au+Au collisions at $\sqrt{s_{NN}} = 20, 62, 130,$ and 200 GeV [25]. The main detector was the time-projection chamber (TPC) located in a solenoidal magnetic field. The magnetic field was 0.25 T for the 20- and 130-GeV data and 0.5 T for the 62- and 200-GeV data. Tracks from the TPC with $0.15 \text{ GeV}/c \leq p_t \leq 2.0 \text{ GeV}/c$ with $|\eta| < 1.0$ were used in the analysis. All tracks were required

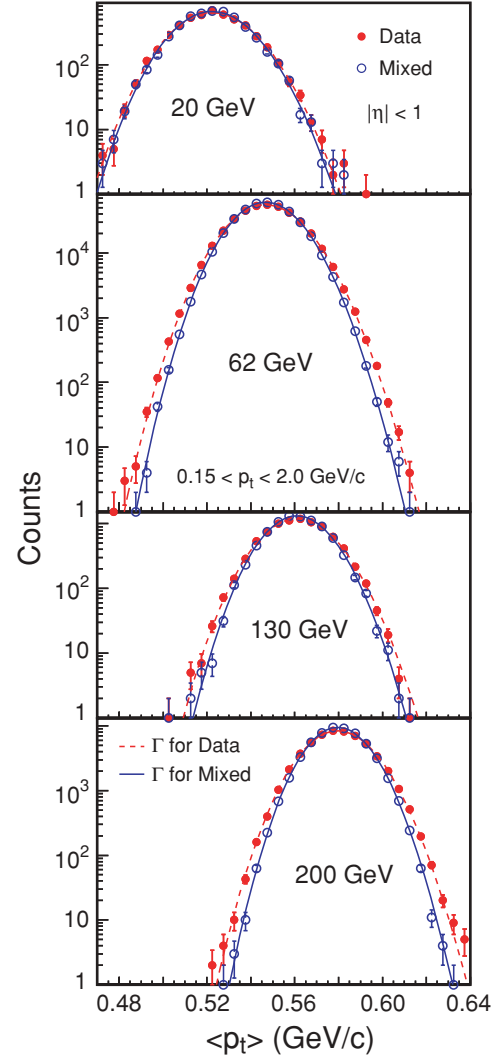


FIG. 1. (Color online) Histograms of the average transverse momentum per event for Au+Au at $\sqrt{s_{NN}} = 20, 62, 130,$ and 200 GeV for the 5% most central collisions at each energy. Both data and mixed events are shown for each incident energy. The lines represent gamma distributions.

to have originated within 1 cm of the measured event vertex. Events were selected according to their distance of the event vertex from the center of STAR. Events were accepted within 1 cm of the center of STAR in the plane perpendicular to the beam direction. For the 20- and 130-GeV data sets, events were accepted with vertices within 75 cm of the center of STAR in the beam direction, whereas for the 62- and 200-GeV data sets, events were accepted within 25 cm of the center.

Data shown for 62, 130 and 200 GeV are from minimum bias triggers. Minimum bias triggers were defined by the coincidence of two zero-degree calorimeters (ZDCs) [26] located ± 18 m from the center of the interaction region. For 20 GeV, a combination of minimum bias and central triggers was used. Centrality bins were determined by use of the multiplicity of all charged particles measured in the TPC with $|\eta| < 0.5$. The centrality bins were calculated as fractions of this multiplicity distribution starting with the

highest multiplicities. The ranges used were 0%–5% (most central), 5%–10%, 10%–20%, 20%–30%, 30%–40%, 40%–50%, 50%–60%, 60%–70%, and 70%–80% (most peripheral). Each centrality was associated with a number of participating nucleons, N_{part} , by use of a Glauber Monte Carlo calculation [27].

We treated the variation of $\langle\langle p_t \rangle\rangle$ within a given centrality bin by using the following procedure. We calculated $\langle\langle p_t \rangle\rangle$ as a function of N_{ch} , the multiplicity used to define the centrality bin. We fitted this dependence and used the fit in Eqs. (1)–(4) on an event-by-event basis as a function of N_{ch} . This method removes the dependence of the experimental results on the size of the centrality bin and slightly reduces $\langle\Delta p_{t,i} \Delta p_{t,j}\rangle$ by removing correlations induced by the changing of $\langle\langle p_t \rangle\rangle$ within the experimental centrality bins. The results presented in this paper were obtained by use of this fitting procedure.

Figure 1 shows histograms of $\langle p_t \rangle$ for the 5% most central Au+Au collisions at 20, 62, 130, and 200 GeV. Histograms for $\langle p_t \rangle$ are also shown for mixed events. The histograms for the data are wider than the histograms for mixed events, indicating that we observe nonstatistical fluctuations at all four incident energies. Similar results are obtained for all centralities. The overall normalization reflects the number events taken at each energy. The values of p_t included in these histograms are not corrected for experimental momentum resolution, acceptance, or efficiency.

We created the mixed events at each energy by randomly selecting one track from an event chosen from measured events in the same centrality and event vertex bin. Ten centrality bins and either 5 or 10 bins (depending on the available number of events at each energy) in the event vertex position in the beam direction were used to create mixed events with the same multiplicity distribution as that of the real events. Note that we do not use mixed events for the quantitative analysis based on $\langle\Delta p_{t,i} \Delta p_{t,j}\rangle$.

The lines in Fig. 1 represent gamma distributions for both the data and mixed events. The parameters for the gamma distributions are shown in Table I. According to Ref. [28], without p_t cuts, the parameter α divided by the average multiplicity in the centrality bin, $\langle N \rangle$, should be approximately two and the parameter β multiplied by $\langle N \rangle$ should reflect the temperature parameter of the p_t distributions. We find that

TABLE I. Parameters for the gamma distributions shown in Fig. 1. The gamma distribution is given by the form $f(x) = \{x^{\alpha-1} e^{-x/\beta} / \Gamma(\alpha) \beta^\alpha\}$ where $\alpha = (\mu^2 / \sigma^2)$ and $\beta = (\sigma^2 / \mu)$ in GeV/c; μ is the mean in GeV/c; and σ is the standard deviation in GeV/c.

Case	α	β	μ	σ
20 GeV, real	1096	4.772×10^{-4}	0.5228	0.01579
20 GeV, mixed	1199	4.360×10^{-4}	0.5227	0.01510
62 GeV, real	1445	3.786×10^{-4}	0.5471	0.01439
62 GeV, mixed	1743	3.139×10^{-4}	0.5470	0.01310
130 GeV, real	1556	3.608×10^{-4}	0.5614	0.01423
130 GeV, mixed	1917	2.927×10^{-4}	0.5612	0.01282
200 GeV, real	1853	3.129×10^{-4}	0.5799	0.01347
200 GeV, mixed	2373	2.443×10^{-4}	0.5799	0.01190

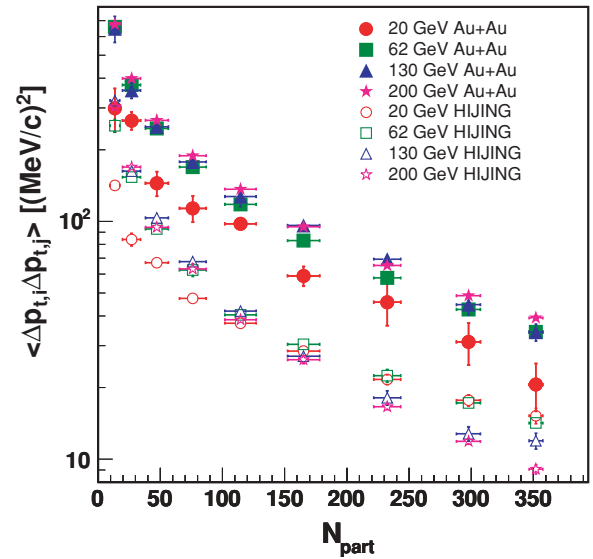


FIG. 2. (Color online) $\langle\Delta p_{t,i} \Delta p_{t,j}\rangle$ as a function of centrality and incident energy for Au+Au collisions compared with HIJING results.

$\alpha/\langle N \rangle$ varies from 2.27 to 1.93 and $\beta\langle N \rangle$ varies from 0.230 to 0.299 GeV/c as the energy goes from 20 to 200 GeV.

To characterize the transverse momentum correlations, we use the quantity $\langle\Delta p_{t,i} \Delta p_{t,j}\rangle$, defined in Eq. (1). Figure 2 shows $\langle\Delta p_{t,i} \Delta p_{t,j}\rangle$ for Au+Au collisions at $\sqrt{s_{NN}} = 20, 62, 130,$ and 200 GeV as functions of centrality. One observes that $\langle\Delta p_{t,i} \Delta p_{t,j}\rangle$ decreases with centrality at all four energies as expected because of a progressive dilution of the correlations resulting from the increased number of participants if the correlations are dominated by pairs of particles that originate from the same nucleon-nucleon collision. The correlations measured at 62, 130, and 200 GeV are similar, whereas the correlations for 20 GeV are smaller than those observed at the higher energies.

To explore the issue of the relative importance of short-range correlations such as Coulomb interactions and Hanbury Brown-Twiss (HBT) effects, we extracted the correlations, excluding pairs with invariant relative momentum q_{inv} , less than 0.1 GeV/c, assuming that all particles were pions. We observed that 10% of the measured correlations at 62, 130, and

200 GeV and 20% of measured correlations at 20 GeV could be attributed to these short-range correlations. These estimates agree with those extracted for 17-GeV Pb+Pb [16] by use of a somewhat different method. We also estimated the contribution of resonances and other charge-ordering effects by studying the reduction in the correlations for same charge (negative) particles compared with correlations for all charged particles. This study indicated that the reduction in $\langle \Delta p_{t,i} \Delta p_{t,j} \rangle$ is 40% at 20 GeV, 20% at 62 and 130 GeV, and 15% at 200 GeV. We do not correct $\langle \Delta p_{t,i} \Delta p_{t,j} \rangle$ for short-range correlations or resonance contributions.

The errors shown in all figures are statistical unless otherwise noted. We estimate the systematic relative errors for $\langle \Delta p_{t,i} \Delta p_{t,j} \rangle$ by using studies of the effects of p_t -dependent efficiencies (1.2%) and sensitivity to track merging and splitting (1.4%). These values give an overall systematic relative error of 2%. The measured correlations were lowered approximately 3% when the fitting method rather than the binning method was used. The reported values are sensitive to the p_t cuts for kinematic and physics reasons. Using HIJING [29], we observe a 6% increase in correlations when the lower p_t cut is removed. Raising the upper p_t cut increases the correlations. We used $0.15 \text{ GeV}/c \leq p_t \leq 2.0 \text{ GeV}/c$ for all the results reported in this paper. The upper p_t cut was chosen to be consistent with previous work [19,24].

Also shown in Fig. 2 are HIJING calculations for Au+Au collisions at $\sqrt{s_{NN}} = 20, 62, 130, \text{ and } 200 \text{ GeV}$ [29]. We used HIJING version 1.36 with the default options, which include jet quenching. The HIJING results were obtained by the selection of particles with $0.15 \text{ GeV}/c \leq p_t \leq 2.0 \text{ GeV}/c$ with $|\eta| < 1.0$ without further efficiency corrections. HIJING reproduces correlations in $p+p$ and $\alpha+\alpha$ collisions at Intersecting Storage Rings (ISR) energies [30], $p+p$ collisions at RHIC energies, and $p+\bar{p}$ collisions at CERN $p+\bar{p}$ Collider (SpS) energies [31]. We use HIJING to provide a reference that incorporates a superposition of nucleon-nucleon interactions. Any differences between HIJING and the experimental results might signal phenomena unique to nucleus-nucleus collisions. The HIJING calculations exhibit little incident energy dependence and decrease with increasing centrality. The values for $\langle \Delta p_{t,i} \Delta p_{t,j} \rangle$ predicted by HIJING are always smaller than the data.

To address the observed dilution of the correlations with centrality and to check the hypothesis that the correlations scale as inverse multiplicity, we multiply $\langle \Delta p_{t,i} \Delta p_{t,j} \rangle$ by the charged-particle pseudorapidity density at a given centrality, $dN/d\eta$. We use fully corrected values for $dN/d\eta$ from published work [32–34]. The quantity $(dN/d\eta)\langle \Delta p_{t,i} \Delta p_{t,j} \rangle$ then is insensitive to efficiency and is similar to the (efficiency-corrected) quantity $\Delta\sigma_{p_t}$ [19] that STAR reported previously.

In Fig. 3 we show the quantity $(dN/d\eta)\langle \Delta p_{t,i} \Delta p_{t,j} \rangle$ for Au+Au collisions at 20, 62, 130, and 200 GeV as functions of centrality. In this figure the errors include the quoted errors in $dN/d\eta$. This quantity increases with incident energy at all centralities. At each energy this measure of the correlations increases quickly as the collisions become more central and then saturates in central collisions. The behavior of this quantity is similar to that of the quantity $\Delta\sigma_{p_t}$ previously studied by STAR [19]. This saturation might indicate effects

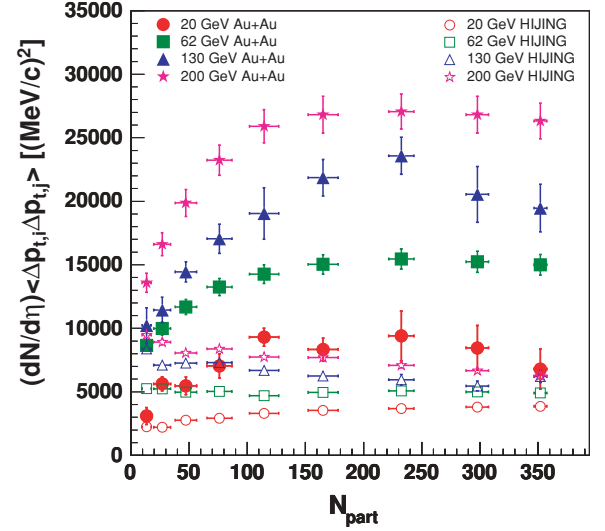


FIG. 3. (Color online) $(dN/d\eta)\langle \Delta p_{t,i} \Delta p_{t,j} \rangle$ as a function of centrality and incident energy for Au+Au collisions compared with HIJING results.

such as the onset of thermalization [15], the onset of jet quenching [14], the saturation of transverse flow [35] in central collisions, or other processes.

In Fig. 3 the results of HIJING calculations for $(dN/d\eta)\langle \Delta p_{t,i} \Delta p_{t,j} \rangle$ are also shown. In contrast to the experimental results, the HIJING results show little dependence on centrality.

To account for possible changes of $\langle \Delta p_{t,i} \Delta p_{t,j} \rangle$ that are due to possible changes in $\langle \langle p_t \rangle \rangle$ with incident energy and/or centrality of the collision, we also study the square root of the measured correlations scaled by $\langle \langle p_t \rangle \rangle$. The resulting quantity $\sqrt{\langle \Delta p_{t,i} \Delta p_{t,j} \rangle} / \langle \langle p_t \rangle \rangle$ is shown in Fig. 4 for Au+Au collisions

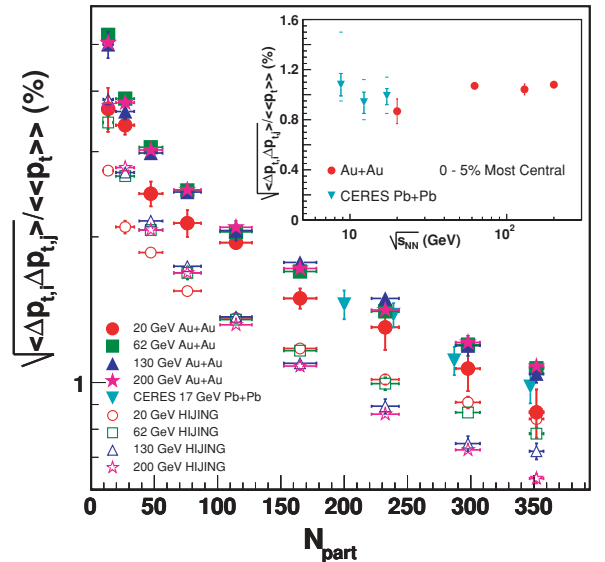


FIG. 4. (Color online) $\sqrt{\langle \Delta p_{t,i} \Delta p_{t,j} \rangle} / \langle \langle p_t \rangle \rangle$ as a function of centrality and incident energy for Au+Au collisions compared with HIJING results for corresponding systems. The inset shows the excitation function for the most central bin.

at 20, 62, 130, and 200 GeV. Similar results from Pb+Pb collisions at 17 GeV [16] are also shown in Fig. 4. These values are consistent with our measured results for Au+Au at 20 GeV. We observe little or no dependence on the incident energy for this quantity. The inset in Fig. 4 demonstrates the incident energy dependence of $\sqrt{\langle\Delta p_{t,i}\Delta p_{t,j}\rangle}/\langle\langle p_t\rangle\rangle$ for the 0%–5% most central bin, in which the Pb+Pb results are from Ref. [16].

In contrast to the measured correlations, HIJING predictions for $\sqrt{\langle\Delta p_{t,i}\Delta p_{t,j}\rangle}/\langle\langle p_t\rangle\rangle$ vary with incident energy. HIJING predicts a different centrality dependence as well as a noticeable dependence on the incident energy.

In conclusion we observe clear nonzero p_t correlations, $\langle\Delta p_{t,i}\Delta p_{t,j}\rangle$ in Au+Au collisions from $\sqrt{s_{NN}} = 20$ to 200 GeV. The quantity $(dN/d\eta)\langle\Delta p_{t,i}\Delta p_{t,j}\rangle$ increases with beam energy. The centrality dependence of $(dN/d\eta)\langle\Delta p_{t,i}\Delta p_{t,j}\rangle$ may show signs of effects such as thermalization [15], the onset of jet suppression [14,24], the saturation of transverse expansion in central collisions [35], or other processes. The quantity $\sqrt{\langle\Delta p_{t,i}\Delta p_{t,j}\rangle}/\langle\langle p_t\rangle\rangle$ shows little or no change with beam energy. HIJING model calculations

underpredict the measured correlations and do not predict the observed centrality dependence.

ACKNOWLEDGMENTS

We thank the RHIC Operations Group and RCF at BNL and the NERSC Center at Lawrence Berkeley National Laboratory for their support. This work was supported in part by the HENP Divisions of the Office of Science of the U.S. Department of Energy; the U.S. National Science Foundation; the Bundesministerium für Bildung, Forschung und Technologie; of Germany; IN2P3, RA, RPL, and EMN of France; Engineering and Physical Sciences Research Council of the United Kingdom; Fundação de Amparo à Pesquisa do Estado de São Paulo of Brazil; the Russian Ministry of Science and Technology; the Ministry of Education and the NNSFC of China; IRP and GA of the Czech Republic; FOM of the Netherlands; DAE, DST, and Council of Scientific and Industrial Research of India; the Swiss National Science Foundation; the Polish State Committee for Scientific Research; and the STAA of Slovakia.

-
- [1] M. Stephanov, K. Rajagopal, and E. Shuryak, Phys. Rev. Lett. **81**, 4816 (1998).
 - [2] M. Stephanov, K. Rajagopal, and E. Shuryak, Phys. Rev. D **60**, 114028 (1999).
 - [3] S. A. Voloshin, V. Koch, and H. G. Ritter, Phys. Rev. C **60**, 024901 (1999).
 - [4] S. A. Bass, M. Gyulassy, H. Stöcker, and W. Greiner, J. Phys. G **25**, R1 (1999).
 - [5] S. Jeon and V. Koch, Phys. Rev. Lett. **85**, 2076 (2000).
 - [6] M. Asakawa, U. Heinz, and B. Müller, Phys. Rev. Lett. **85**, 2072 (2000).
 - [7] S. A. Bass, P. Danielewicz, and S. Pratt, Phys. Rev. Lett. **85**, 2689 (2000).
 - [8] H. Heiselberg, Phys. Rep. **351**, 161 (2001).
 - [9] Z.-W. Lin and C. M. Ko, Phys. Rev. C **64**, 041901(R) (2001).
 - [10] H. Heiselberg and A. D. Jackson, Phys. Rev. C **63**, 064904 (2001).
 - [11] E. V. Shuryak and M. A. Stephanov, Phys. Rev. C **63**, 064903 (2001).
 - [12] C. Pruneau, S. Gavin, and S. Voloshin, Phys. Rev. C **66**, 044904 (2002).
 - [13] M. Stephanov, Phys. Rev. D **65**, 096008 (2002).
 - [14] Q. Liu and T. A. Trainor, Phys. Lett. **B567**, 184 (2003).
 - [15] S. Gavin, Phys. Rev. Lett. **92**, 162301 (2004).
 - [16] D. Adamova *et al.* (CERES Collaboration), Nucl. Phys. **A727**, 97 (2003).
 - [17] M. M. Aggarwal *et al.* (WA98 Collaboration), Phys. Rev. C **65**, 054912 (2002).
 - [18] H. Appelshauser *et al.* (NA49 Collaboration), Phys. Lett. **B459**, 679 (1999).
 - [19] J. Adams *et al.* (STAR Collaboration), Phys. Rev. C **71**, 064906 (2005).
 - [20] J. Adams *et al.* (STAR Collaboration), Phys. Rev. C **68**, 044905 (2003).
 - [21] J. Adams *et al.* (STAR Collaboration), Phys. Rev. Lett. **90**, 172301 (2003).
 - [22] K. Adcox *et al.* (PHENIX Collaboration), Phys. Rev. Lett. **89**, 212301 (2002).
 - [23] K. Adcox *et al.* (PHENIX Collaboration), Phys. Rev. C **66**, 024901 (2002).
 - [24] S. S. Adler *et al.* (PHENIX Collaboration), Phys. Rev. Lett. **93**, 092301 (2004).
 - [25] K. H. Ackermann *et al.* (STAR Collaboration), Nucl. Instrum. Methods A **499**, 624 (2003).
 - [26] C. Adler, A. Denisov, E. Garcia, M. Murray, H. Ströbele, and S. White, Nucl. Instrum. Methods A **461**, 337 (2001).
 - [27] J. Adams *et al.* (STAR Collaboration), Phys. Rev. C **70**, 044901 (2004).
 - [28] M. J. Tannenbaum, Phys. Lett. **B498**, 29 (2001).
 - [29] X. N. Wang and M. Gyulassy, Phys. Rev. D **44**, 3501 (1991).
 - [30] K. Braune *et al.*, Phys. Lett. **B123**, 467 (1983).
 - [31] X. N. Wang and M. Gyulassy, Phys. Rev. D **45**, 844 (1992).
 - [32] B. Back *et al.* (PHOBOS Collaboration), Phys. Rev. C **65**, 061901(R) (2002).
 - [33] B. Back *et al.* (PHOBOS Collaboration), Phys. Rev. Lett. **94**, 082304 (2005).
 - [34] B. Back *et al.* (PHOBOS Collaboration), Phys. Rev. C **70**, 021902 (2004).
 - [35] S. A. Voloshin, nucl-th/0312065 (2004).